ELSEVIER

Journal of Organometallic Chemistry 625 (2001) 200–207

Journal of Organometallic Chemistry

www.elsevier.nl/locate/jorganchem

X-ray structural and Mössbauer spectroscopic investigation of terminal ethynylmetallocenium salts

Herwig Schottenberger [a],*[1], Klaus Wurst [a], Rolfe H. Herber [b],*[2]

[a] *Institut für Allgemeine, Anorganische und Theoretische Chemie, Leopold Franzens Universitaet, Innrain 52a, A-6020 Innsbruck, Austria*
[b] *Racah Institute of Physics, The Hebrew University of Jerusalem, 91904 Jerusalem, Israel*

Received 24 August 2000; received in revised form 30 November 2000; accepted 4 December 2000

Abstract

Oxidation of ethynyloctamethylferrocene (**OMFA**), [**201472-67-5**], with ferrocenium hexafluorophosphate in acetonitrile afforded previously unreported ethynyloctamethylferrocenium hexafluorophosphate salt **1** (**OMFA**$^+$PF$_6^-$).

Temperature-dependent ^{57}Fe Mössbauer effect studies of **1** and neutral **OMFA** have shown a marked difference of behavior in the motion of the metal atom, which can be associated with the onset of ring rotation/libration in the latter at ~248 K, but which is strongly inhibited in **1**.

Supplementary X-ray structure determinations of **1** and ethynylcobaltocenium hexafluorophosphate (**CA**$^+$PF$_6^-$), [**131276-87-4**], a close structural model for the unstable, oxidized form of ferrocenylacetylene (**FA**$^+$), have been performed. The most remarkable structural feature of this stable salt of oxidized cobaltocenylacetylene (**CA**) is its crystal constitution: alternating different cation layers are separated by identical layers of PF$_6^-$ counter ions, thus exhibiting a unique type of lattice internal polymorphism.

Keywords: Ethynyl-metallocenes; Acetylenes; X-ray structure; Mössbauer spectroscopy; Metal atom motion

1. Introduction

Terminal metallocene-substituted acetylenes, especially the members of highly methylated ferrocenes [1,2], represent relevant synthons for the design of electronically coupled [3] dimers [4], oligomers [5], polymers with conjugated backbones [6], and redox-tunable (or switchable) auxiliaries in molecular composites [7].

Moreover, some unique features related to the structural and conformational details, as well as the electronic properties of ethyne-derived metallocenes [8], justify a detailed investigation of the parent monomers in addition to their routine analytical characterization.

A technique which has shown itself to be particularly useful in characterizing some of the dynamical aspects of such iron-metallocenes is temperature-dependent ^{57}Fe Mössbauer spectroscopy, which can also serve to elucidate the variations in the electron density around the metal atom, as well as providing information concerning the symmetry of the charge distribution. In particular, it has recently been reported [9] that a number of octamethyl ferrocenes display evidence for anomalous metal atom motion in the solid state, and the present investigation extends these observations to octamethylethynyl ferrocene (**OMFA**), [**201472-67-5**], its PF$_6^-$ salt **1** and the related ferrocenylacetylene monomer (**FA**), [**1271-47-2**], illustrating the complementarity of these and single-crystal X-ray diffraction methods.

2. Results and discussion

2.1. 1-Ethynyl-1′,2,2′,3,3′,4,4′,5-octamethylferrocenium hexafluorophosphate (1)

2.1.1. Mössbauer spectroscopic investigation

In contrast to the normal doublet Mössbauer spectra observed for neutral ferrocene- related complexes such

---

[1] *Corresponding author. E-mail: herwig.schottenberger@uibk.ac.at

[2] Corresponding author. Tel.: +972-2-6584 244; fax: +972-2-6586 347; e-mail: herber@vms.huji.ac.il

0022-328X/01/$ - see front matter © 2001 Elsevier Science B.V. All rights reserved.
PII: S0022-328X(01)00646-5

as octamethylferrocene [1], those of the cationic complex (**OMFA**$^+$PF$_6^-$, **1**) consist of broadened lines characteristic of spin-lattice relaxation in the solid. A typical spectrum (which evidences a small amount of an impurity) is shown in Fig. 1. Representative relaxation rates, calculated from the ^{57}Fe Mössbauer spectra are 2.3×10^{10} s^{-1} at 90 K and 5.5×10^{-10} s^{-1} at 280 K, and are somewhat faster than those reported earlier [10] for related ferrocenium complexes. The isomer shift (IS), quadrupole splitting (QS) and associated temperature-dependent parameters are summarized in Table 1. The IS at 90 K for **1** is very similar to those observed for related ferrocenium complexes [9,10], reflecting the strong covalency of the metal atom–cyclopentadienyl bonding interaction, and its insensitivity to the presence of the alkyl ring substituents. The almost total collapse of the QS parameter, resulting from the removal of a single electron, reduces this hyperfine interaction by a factor of ~15 relative to the neutral parent, in consonance with the related observations in ferrocene and ferrocenium complexes. This reduction in the QS has been discussed by Collins [11] on the basis of the molecular orbital model of Dahl and Ballhausen [12]. The reduction of the IS on oxidation of OMFA to **OMFA**$^+$PF$_6^-$ (**1**) is smaller than that reported for the analogous ferrocene parent, but is consistent with the removal of 3-d electron density.

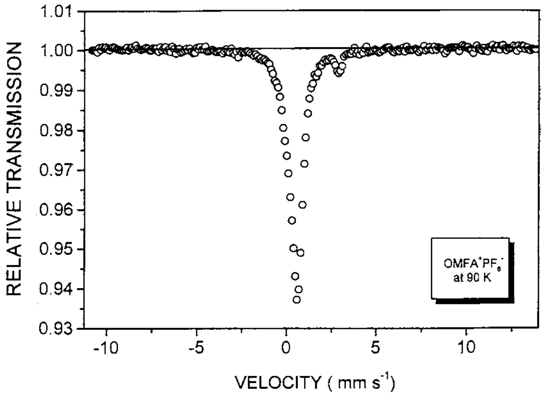

Fig. 1. ^{57}Fe Mössbauer Spectrum of **OMFA**$^+$PF$_6^-$ at 90 K. There is a small impurity peak at ~2.7 mm s^{-1}, but the presence of this absorbance has been corrected for in the data analysis discussed in the text. The velocity scale is with respect to the centroid of an α-Fe absorption spectrum at room temperature.

Table 1
Mössbauer data for the compounds discussed in the text

Compound	**OMFA** +PF$_6^-$ (**1**)	**OMFA**	**FA** (Ref. [1])	Units
IS(90)	0.496(1)	0.507(2)	0.524(3)	mm s^{-1}
QS(90)	0.154(1)	2.411(1) [b]	2.343(1)	mm s^{-1}
$-$dIS/dT	3.50(23)	3.15(16)	3.86(9)	mm s^{-1} × 10^{-4}
$-$d ln A/dT	9.2(9) [a]	8.7(4)	7.0(2)	K^{-1} × 10^{-3}
M_{eff}	119	132	108	Daltons
T_{M}	84.4	82.2	102	K
T_{mp}		436	325	K

[a] $230 \leq T \leq 320$ K.

[b] The QS has a minimum value [2.391(1) mm s^{-1}] at ~200 K.

As has been observed previously [10] in related ferrocenium complexes, the temperature dependence of the IS of **1** is negative, and very similar to that in parent **OMFA**. The 'effective vibrating mass' [13,14] calculated for **1** from these data is 119 Da, and this value compared to the 'bare' ^{57}Fe mass again reflects the covalent bonding of the metal atom to the cyclopentadienyl ligands. The temperature dependence of the QS is very weakly negative, and is unremarkable.

On the other hand, the temperature dependence of ln A (A = area under the resonance curve), which is related to the mean-square-amplitude of vibration (msa) of the metal atom, is very different for **1** and for **OMFA**, as reflected in Fig. 2. As has been reported previously [15,16], for ferrocene-derived complexes in which there are a limited number of ring substituents [e.g. ferrocenylacetylene (**FA**), and 1,1′-dimethylferrocene], the resonance effect is observable to within 0.5° of the melting point. In contrast, the resonance effect observed for the neutral complex **OMFA** effectively vanishes some 180° below the melting point, an effect which has also been reported [9] for octamethylferrocene (OMF), octamethyl ethenyl ferrocene (OMFE) and nonamethyl ferrocene (NMF). These observations have been ascribed to the onset of ring rotation and libration in those compounds where there is at least one ring C–H bond present in conjunction with a fully (or almost fully) ring substituted moietie. Under the reasonable assumption that the ln $A(T)$ behavior observed for **OMFA** has its origin in the same kind of onset of ring rotation and libration at about 248 K, the ln $A(T)$ behavior of **1**, summarized in Fig. 2, strongly suggests that the presence of the PF$_6^-$ anions in the structure markedly inhibit the onset of this kind of ring motion in the cationic portion of the complex.

The question which immediately arises relates to the uniquenes of the structure of **1** and **OMFA** as well as those of octamethyl ferrocene (OMF), nonamethyl ferrocene (NMF) and octamethyl-ethenylferrocene (OMFE) which would account for these observations related to the mean-square-vibrational amplitude of the iron atom, in contrast to those ferrocenes in which this effect is not observed. A plausible origin of the large msav in **OMFA** above ~248 K is that the onset of ring rotation also causes a ring libration, arising from a 'gear-wheel effect' due to the presence of one ring site which has a C–H bond rather than a C–CH$_3$ sub-

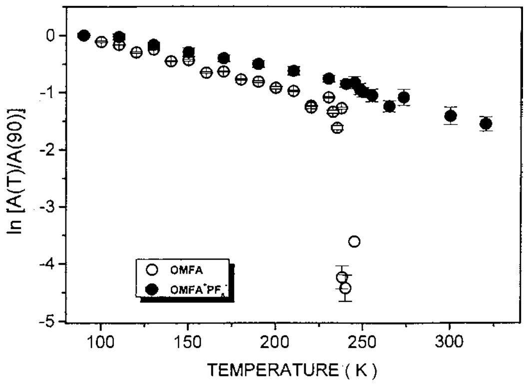

Fig. 2. Temperature dependence of the logarithm of the area under the resonance curve (normalized to the 90 K datum) for **OMFA** and **OMFA**$^+$PF$_6^-$. The 'break' in the **OMFA** data occurs some 180° below the melting point.

stituent. This libration results in a large increase in the msav of the metal atom and the consequent large reduction in the recoil-free fraction of the Mössbauer atom in the structure. One of the consequences of this behavior is that the structure of **OMFA** must be disordered above the temperature at which ring rotation/libration begins. In this context it should be noted that it has not been possible [17a] to acquire suitable X-ray diffraction data on this compound at room temperature — the diffraction data reported in this study (see Table 2) were obtained at 218(2) K, well below the transition temperature of 248 K extracted from the Mössbauer spectroscopic results. The details of the X-ray diffraction data are discussed more fully below.

2.1.2. X-ray structural investigations

Ethynyl-octamethylferrocenium hexafluorophosphate (**1**) crystallizes in the centrosymmetric space group *C*2/*c*. The crystals are made up of cationic ferrocene layers perpendicular to the *a*-axis, intercalated by anion layers, consisting of two different PF$_6^-$ types. The molecular structure of **1** is shown in Fig. 3, in which the bold lines between the phosphorus and fluorine atoms of the anion reflect the disorder present in this part of the molecule.

The crystal lattice structure of **1** is shown in Fig. 4. The crystal architecture reflects no significant spatial fluorine-proton interactions, as evidenced by the absence of any remarkable alterations of the standard bond lengths (triple bond 116.8(5) pm) and distances between closest neighbors; e.g. the closest distance between methyl protons (226.1 pm) is smaller than the closest acetylenic proton–fluorine distance (232.8 pm) and, as expected, the sterically shielded Cp–proton–F distance (245.6 pm), respectively. The fluorine atoms of the hexafluorophosphate ions exhibit varying degrees of disorder (see the bold line connections for the disordered positions of the PF$_6^-$ anions in Fig. 4).

2.2. *Ethynylcobaltocenium hexafluorophosphate **[131276-87-4]***

2.2.1. *Lattice internal layer polymorphism of **[131276-87-4]** (CA$^+$PF$_6^-$–)*

In ethynylcobaltocenium hexafluorophosphate (**2**) Fig. 5, the fluorine atoms show similar varying degrees of disorder.

Table 2
Crystal data and structure refinement for 1 and [131276-87-4]

Ethynylmetallocenium salt	**1**	[**131276-87-4**]
Molecular formula	$C_{20}H_{26}Fe^+PF_6^-$	$C_{12}H_{10}Co^+PF_6^-$
Formula wweight	467.23	358.10
Crystal system	Monoclinic	Monoclinic
Space group	*C*2/*c* (no.15)	*P*2$_1$/*c* (no. 14)
Unit cell dimensions		
a (pm)	3377 (2)	1455.29(6)
b (pm)	839.6(2)	1225.94(6)
c (pm)	1645.8(2)	1528.67(8)
α (°)	90	90
β (°)	112.94(2)	101.397(3)
γ (°)	90	90
Vol (nm^3)	4297(3)	2.6735(2)
Z	8	8
Temperature (K)	218(2)	218(2)
Density (calc) (Mg m^{-3})	1.444	1.779
Absorption coefficient (mm^{-1})	0.829	1.458
F(000)	1928	1424
Color, habit	Blue–green plate	Light yellow prism
Crystal size (mm)	0.6 × 0.4 × 0.06	0.25 × 0.15 × 0.05
θ Range for data collected (°)	2.51–24.00	1.43–22.50
Index ranges	$0 \le h \le 38$; $-1 \le k \le 9$; $-18 \le l \le 17$	$0 \le h \le 17$; $0 \le k \le 14$; $-18 \le l \le 17$
No. of reflections collected	3953	6744
No. of independent reflections	3370 ($R_{int} = 0.0281$)	3492 ($R_{int} = 0.0294$)
No. of reflections with $I > 2\sigma(I)$	2596	2745
Absorption correctiorr	ψ-scan	None
Max and min transm	1.000 and 0.853	0.964 and 0.859
Refinement method	Full-matrix least-squares on F^2	Full-matrix least-squares on F^2
Data/restraints/parameters	3170/0/318	3306/0/423
Goodness-of-fit on F^2	1.040	1.097
Final *R* indices [$I > 2\sigma(I)$]	$R_1 = 0.0389$; $wR_2 = 0.0898$	$R_1 = 0.0474$; $wR_2 = 0.1108$
R indices (all data)	$R_1 = 0.0600$; $wR_2 = 0.1006$	$R_1 = 0.0664$; $wR_2 = 0.1295$
Extinction coefficient	0.00076(10)	
Largest difference peak and hole (e nm^{-3})	349 and −278	566 and −290

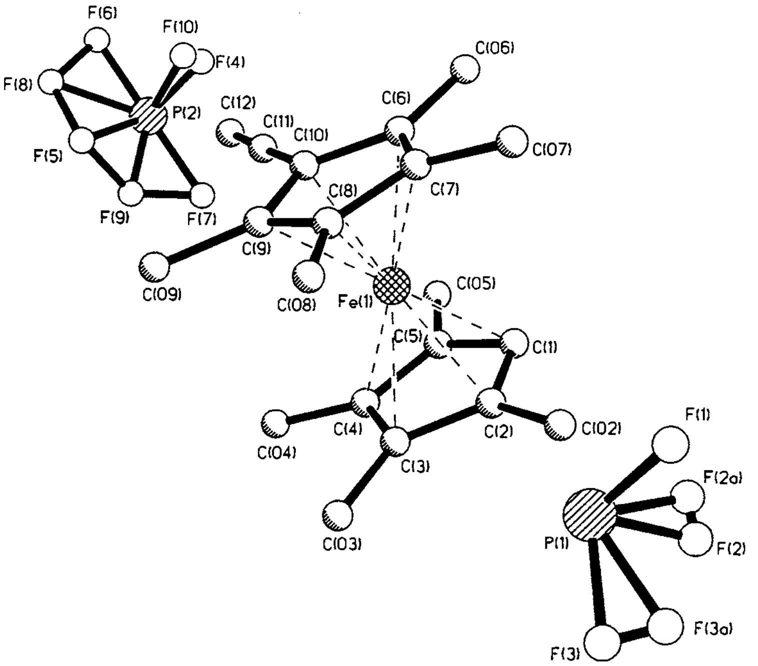

Fig. 3. Moleculer structure of **1** (**OMFA**$^+$PF$_6^-$). The bold lines between the P and F atoms connect disorder positions.

The compound crystallizes in the centrosymmetric space group $P2_1/c$, with two independent molecules in the asymmetric unit. Again, perpendicular to the a-axis, layers of the metallocene cations are separated by anion layers with two different types of PF$_6^-$ anions. Within the lattice, the repeating anion layer types are identical as such, but in contrast to the anionic intercalates, the cobaltocenium molecules are incorporated as two periodically alternating quasipolymorphic layers within one crystal. When every second row of the second layer is shifted along the c-axis for half a lattice constant, the resulting layer is nearly identical with the first layer (see packing plots for Co1 and Co2, Figs. 6 and 7, respectively).

The observed difficulty in growing single crystals suitable for X-ray diffraction may also be attributed to the complexity of this crystal formation. Spatial fluorine–proton interactions do not seem to contribute significantly to lattice-determining crystal forces, since no unexpected distances between closest neighbors are observable. The shortest distance between fluorine and a Cp-proton is 231.7 pm, and that between fluorine and an ethyne proton is 237.5 pm, respectively.

3. Conclusions and comparison

Mössbauer data for **1** over the temperature range $90 \leq T \leq 320$ K have been analyzed in terms of a paramagnetic metal center which shows typical spin-lattice relaxation, in consonance with earlier studies of related ferrocenium complexes [9,10]. Comparison of the recoil-free fraction results (as reflected in the normalized areas under the resonance curves) of **1** and **OMFA**, in conjunction with the corresponding X-ray diffraction data, vide infra, suggest that the onset of

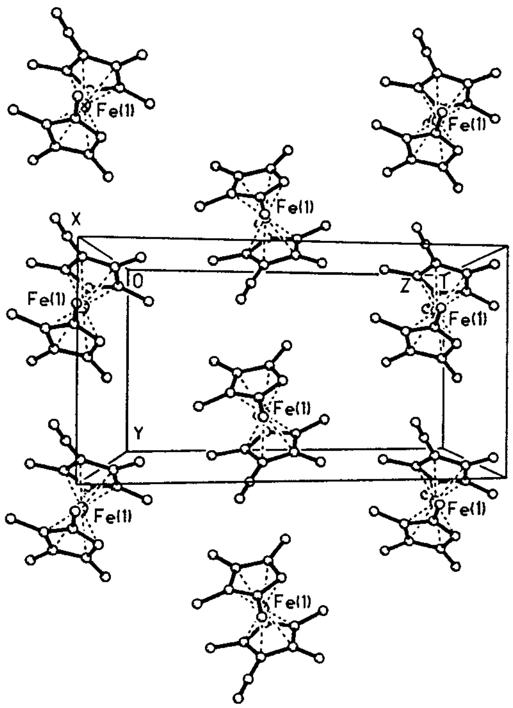

Fig. 4. Crystal lattice with the unit cell of **1** (**OMFA**$^+$PF$_6^-$). The anions are omitted for clarity.

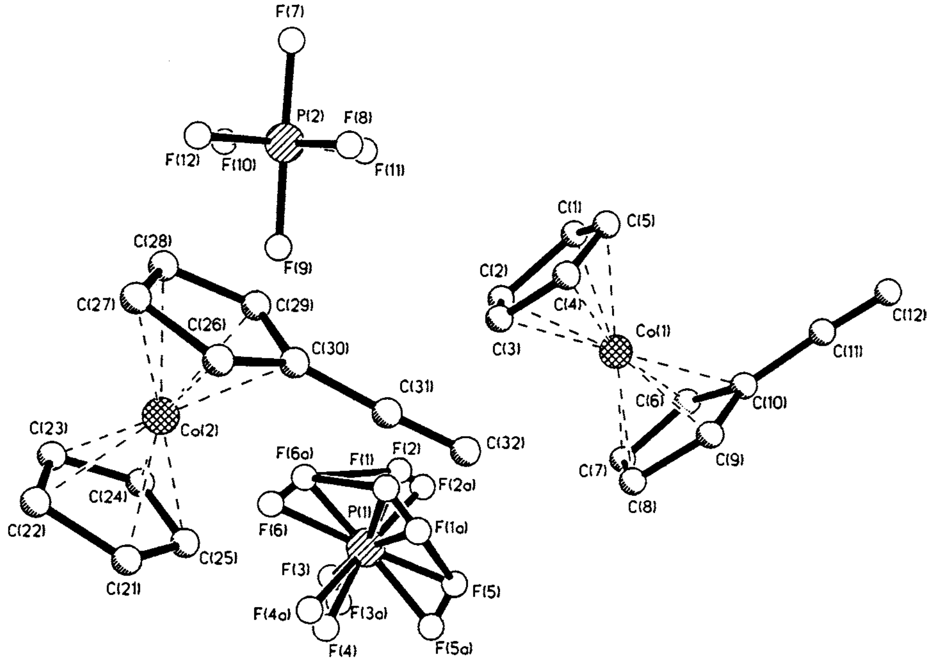

Fig. 5. Molecular structure of [**131276-87-4**] (**CA**$^+$PF$_6^-$). The bold lines between the P and F atoms connect disorder positions.

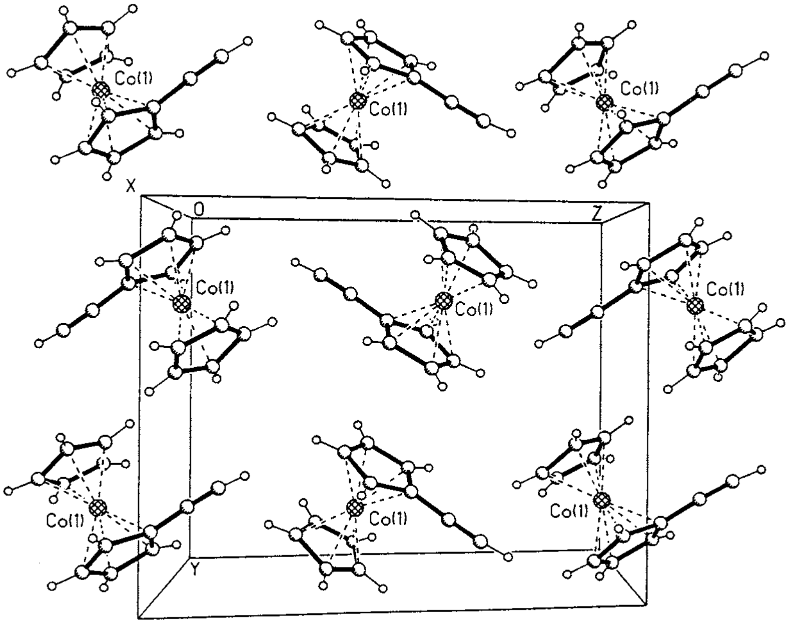

Fig. 6. First cation lattice layer (**Co1**) with the unit cell of **CA**$^+$PF$_6^-$. The anions are omitted for clarity.

ring rotation/libration, observed in **OMFA** at ~ 248 K, is inhibited in the cationic complex up to temperatures of at least 320 K. These observations are directly related to the presence of long-range order in **1** at room temperature, which does not obtain for **OMFA**, negating all efforts to obtain diffractable crystals of the latter at ~ 290 K. That these observations originate in the presence of an octamethyl Cp ring structure in **OMFA** is confirmed by the results obtained for the related ethynylferrocene (**FA**), which have been reported earlier [1].

In contrast to cobaltocenes, terminal cationic ethynylferrocenes are only stable if they are stabilized by high alkyl-substitution, since — formally as their canonical forms, the respective α-vinyl radical cations — they are prone to further conversions via various addition, resp. substitution, pathways [18]. Thus, they undergo (spontaneous) conversions such as additions and substitutions, and are therefore not isolatable. This may be the main reason why only cyclovoltammetric characterizations of the parent ethynyl-ferrocene/ferrocenium couple (FA/FA$^+$), and even of the ethynyl-pentamethylferrocene/ferrocenium couple (PMFA/PMFA$^+$), have so far been reported [18,19]. Thus, regarding structural comparisons, ethynylcobaltocenium salts may serve as close model supplements for the ferrocene series.

According to conclusions based on Mössbauer measurements [17b], it is not possible to grow or diffract disorder free single crystals of ethynyl-octamethylferrocene under practical (ambient temperature) conditions.

Considering the acetylynic bond lengths (by X-ray analysis) for elucidation of the ligand electron density is not an appropriate method of choice. The triple bond lengths were found to be within the expected range around 117 pm (for details, vide infra), and do not deviate dramatically from the neutral homologues. As a point of reference, the three different members of the unit cell of (neutral) ethynylferrocene [20] are also within the same range (116.5(14), 117(2), resp. 118(2) pm); on the other hand, trimethylsilyl-substitution causes a bond elongation to 118.9(7) pm [8].

In this context, it is noteworthy that the triple bond length in the first cobaltocenium layer of the hexafluorophosphate salt of this very stable oxidized form of cobaltocenylacetylene, (**CA$^+$PF$_6^-$**) is, within experimental error, identical ($C_{CA1}11-C_{CA1}12 = 116.8(9)$ pm) with the distance found in the ethynyl-octamethylferrocene salt (**OMFA$^+$PF$_6^-$**), **1**, ($C_{OMFA}11-C_{OMFA}12 = 116.8(5)$ pm), while the triple bond in the second cobaltocenium layer is slightly different ($C_{CA2}31-C_{CA2}32 = 117.6.(9)$ pm). Thus, bond lengths seem rather independent of charge, resp. electron density, induced by the metallocene, but they may — besides extreme (sterically demanding) substitution patterns — be altered predominantly by terminal acetylenic interactions, i.e. hydrogen bridges, or through space influences by crystal packing requirements and the like.

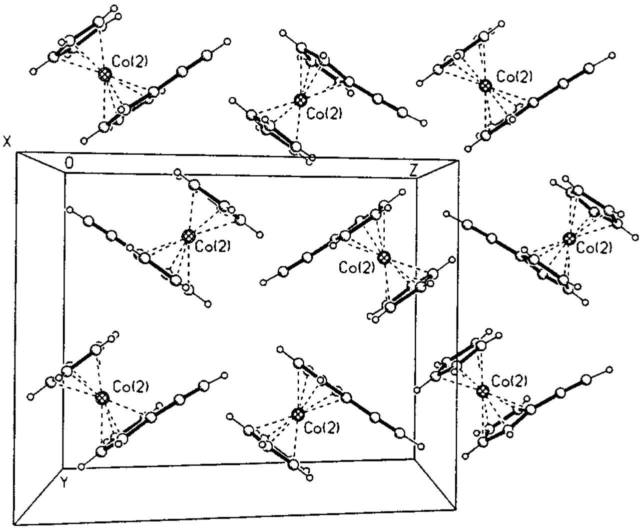

Fig. 7. Second cation lattice layer (**Co2**) with the unit cell of **CA$^+$PF$_6^-$**. The anions are omitted for clarity.

4. Experimental

All starting compounds not referenced (e.g. ferrocenium hexafluorophosphate, [**11077-24-0**]), are commercially available. Purchased starting materials were used without any further treatment, except acetonitrile (HPLC grade), which was deoxygenated ultrasonically while purging with argon for 3 min before use.

The precursor of **1**, the neutral parent compound, 1 - ethynyl - 1′,2,2′,3,3′,4,4′,5 - octamethylferrocene, [**201472-67-5**], was prepared according to the convenient one-pot procedure published by Jutzi and Kleinebekel [5].

A modified protocol also starts from octamethylferrocene carbaldehyde [**128925-12-2**], but, by the isolation of the intermediate Wittig isomers, (*E*,*Z*)-1-chloro-2-1′,2,2′,3,3′,4,4′,5-octamethylferrocenyl)ethenes, some higher yields (92%, resp. 97% of theory) may be obtained [21].

Ethynylcobaltocenium hexafluorophosphate, [**131276-87-4**], was prepared according to the published procedure [22].

4.1. Instrumentation

Nicolet 510 FT-IR (IR); Varian CH-7 (MS); Siemens P4 (X-ray). Microanalyses of **1** were obtained from the Analytical Department of Lenzing AG, A-4840 Lenzing, Austria, and were found to be consistent with the theoretical value.

The Mössbauer spectrometer, its method of calibration, the method of data reduction and thermal control have been described earlier [23]. All isomer shifts are reported with respect to the centroid of an α-Fe spectrum at room temperature (r.t.). The details of the relaxation spectra analysis have also been described earlier [9]. The microcrystalline samples were well mixed with BN to minimize preferential crystal orientation effects, and then mounted in plastic sample holders in the spectrometer. All samples were optically ‘thin’, and no saturation effects were applied to the data.

*4.2. 1-Ethynyl-1′,2,2′,3,3′,4,4′,5-octamethylferrocenium hexafluorophosphate (**1**)*

1 - Ethynyl - 1′,2,2′,3,3′,4,4′,5 - octamethylferrocene (0.100 g, 0.31 mmol) was dissolved in 4 ml of deoxygenated CH_3CN at r.t. Subsequently, ferrocenium hexafluorophosphate (0.100 g, 0.30 mmol), was added in one portion. The resulting heterogeneous reaction mixture was immersed in an ultrasonic bath for 3 min, and a green solution formed. After 3 min, 20 ml of diethyl ether was added to precipitate crude **1**. The resulting green suspension was centrifuged and the slightly green supernatant, containing the reduced neutral ferrocene, was discarded. The solid remainder was resuspended in ether (7 ml) and centrifuged until the supernatant was colorless (three times). The green solid was dried under vacuum, yielding 0.104 g of pure **1** (according to TLC; silica, eluent: dichloromethane–acetonitrile, 1:3 v/v) as air-stable green amorphous powder; yield: 72% of theory. Recrystallization from ethereal dichloromethane affords a crystalline product.

Analytical data: $C_{20}H_{26}\ Fe^{+}PF_6^{-}$, $M = 467.23$ g mol^{-1} (cation 322.27 g mol^{-1}).

M.p.(by Kofler hot-plate apparatus): continuous decomposition at elevated temperatures, and on storage over prolonged periods at ambient conditions.

MS (FAB pos.): exact mass calc. (cation): 322.14 g mol^{-1}; m/z found = 322.17 g mol^{-1} (M^{+}, 100%).

*4.3. X-ray measurement and structure determination of **1** and [**131276-87-4**]*

Single crystals of **1** and [**131276-87-4**], suitable for X-ray analysis, were obtained by slow crystallization from dichloromethane–diethyl ether.

For compound **1**, a Bruker P4 diffractometer with graphite-monochromatized $Mo-K_{\alpha}$ radiation ($\lambda = 71.073$ pm) was used for data collection. Intensities were measured via ω-scans and corrected for Lorentz and polarization effects. Compound **2** was measured on a Nonius Kappa CCD area-detector diffractometer ($\lambda = 71.073$ pm) with the CCD detector placed 36 mm from the crystal via a mixture of $2°\phi$ and ω-scans. The raw data were processed with the program DENZO-SMN [24] to obtain conventional data.

The structures were solved by direct methods (SHELXS-86) [25] and refined by full-matrix least-squares against F^2 (SHELXL-93) [26]. The function minimized was $\Sigma[w(F_o^2 - F_c^2)^2]$ with the weight defined as $w^{-1} = [\sigma^2(F_o^2) + (xP)^2 + yP]$ and $P = (F_o^2 + 2F_c^2)/3$. All non-hydrogen atoms were refined with anisotropic displacement parameters. The hydrogen atoms at the ethynyl groups were refined isotropically, all other hydrogen atoms were located by difference Fourier methods, but in the refinement they were generated geometrically and refined with isotropic displacement parameters 1.2 times and 1.5 (for the methyl-group) higher than $U_{eq.}$ of the attached carbon atoms. In compound **1**, with two half counter ions in the asymmetric unit, the PF_6-ions were disordered. One, with P(1) in an inversion center, with the occupancy of 0.6:0.4, the other, with P(2) on a twofold axis, with 0.8:0.2. In compound **2** there are two molecules in the asymmetric unit and only one of the counter ions is disordered with the occupancy of 0.66:0.33.

Further crystallographic data are collected in Table 2.

Acknowledgements

This work was supported in part by The Israel National Science Foundation. The authors are indebted to Prof. I. Nowik for help with the Mössbauer data reduction. We are also grateful to Dr. Thomas Baldinger, and Dr. Walter Muehlecker, Lenzing AG, for performing the elemental analyses, and recording the mass spectrum of **1**, respectively.

References

[1] H. Schottenberger, M.R. Buchmeiser, R.H. Herber, J. Organomet. Chem. 612 (2000) 1.
[2] M.R. Buchmeiser, A. Hallbrucker, I. Kohl, N. Schuler, H. Schottenberger, Designed Monomers and Polymers 3 (2000) 421.
[3] S. Barlow, D. O'Hare, Chem. Rev. 97 (1997) 637 and references cited therein.
[4] Y. Suzuki, R. Hirotani, H. Komatsu, H. Yamazaki, Chem. Lett. 12 (1999) 1299.
[5] P. Jutzi, B. Kleinebekel, J. Organomet. Chem. 545-546 (1997) 573.
[6] H. Schottenberger, M.R. Buchmeiser, Recent Res. Dev. Macromol. Res. 3 (2) (1998) 535.
[7] U. Siemeling, U. Vorfeld, B. Neumann, H.G. Stammler, P. Zanello Piero, F. Fabrizi De Biani, Eur. J. Inorg. Chem. (1999) 1.
[8] M.R. Buchmeiser, H. Schottenberger, K. Wurst, J. Organomet. Chem. 584 (1999) 301.
[9] I. Nowik, R.H. Herber, Inorg. Chim. Acta 310 (2000) 191.
[10] R.H. Herber, T. Hanusa, Hyperfine Interact. 108 (1997) 563.
[11] R.L. Collins, J. Chem. Phys. 42 (1965) 1072.
[12] See the discussion in: N.N. Greenwood, T.C. Gibb, Mössbauer Spectroscopy, Chapman and Hall, London, 1971, pp. 233 ff and references therein.
[13] R.H. Herber (Ed.), Chemical Mössbauer Spectroscopy, Plenum Press, New York, 1984.
[14] (a) G. Long, H. Dautot, F. Grandjean, G.P. Meisner, D.T. Morelli, Phys. Rev. B 62 (2000) 6829. (b) H.R. Rechenberg, Phys. Rev. B 62 (2000) 6827.
[15] R.H. Herber, I. Nowik, Hyperfine Interact. 126 (2000) 127.
[16] R.H. Herber, Inorg. Chim. Acta 291 (1999) 74.
[17] (a) H. Schottenberger, K. Wurst, private communication. (b) R.H. Herber, private communication.
[18] H. Nock, H. Schottenberger, J. Org. Chem. 58 (1993) 7045.
[19] B. Bildstein, A. Hradsky, H. Kopacka, R. Malleier, K.H. Ongania, J. Organomet. Chem. 540 (1997) 127.
[20] K. Wurst, O. Elsner, H. Schottenberger, Synlett (1995) 833.

[21] N. Schuler, PhD Thesis, University of Innsbruck, Innrain 52a, A-6020 Innsbruck, Austria, 1998, p. 104.
[22] M. Wildschek, C. Rieker, P. Jaitner, H. Schottenberger, K.E. Schwarzhans, J. Organomet. Chem. 396 (1990) 355.
[23] R.H. Herber, B. Bildstein, P. Denifl, H. Schottenberger, Inorg. Chem. 36 (1997) 3586.
[24] Z. Otwinowski, W. Minor, in: C.W. Carter Jr., R.M. Sweet (Eds.), Methods in Enzymology, vol. 276, Academic Press, New York, 1996, pp. 307–326.
[25] G.M. Sheldrick, SHELXS-86: Program for Crystal Structure Solutions, University of Göttingen, Germany, 1986.
[26] G.M. Sheldrick, SHELXL-93: Program for the Refinement of Crystal Structures, University of Göttingen, Germany, 1993.